Title

α-synuclein aggregates induce c-Abl activation and dopaminergic neuronal loss by a feed-forward redox stress mechanism

Authors

Ghosh, Soumitra
Won, Seok Joon
Wang, Jiejie
et al.

Publication Date

2021-07-01

DOI

10.1016/j.pneurobio.2021.102070

Peer reviewed

Progress in Neurobiology xxx (xxxx) 102070

Contents lists available at ScienceDirect

Progress in Neurobiology

journal homepage: www.elsevier.com/locate/pneurobio

Original Research Article

α-synuclein aggregates induce c-Abl activation and dopaminergic neuronal loss by a feed-forward redox stress mechanism

Soumitra Ghosh [a, b], Seok Joon Won [a, b], Jiejie Wang [a, b], Rebecca Fong [a, b], Nicholas J.M. Butler [a, b], Arianna Moss [a, b], Candance Wong [a, b], June Pan [a, b], Jennifer Sanchez [a, b], Annie Huynh [a, b], Long Wu [a, b], Fredric P. Manfredsson [c], Raymond A. Swanson [a, b, *]

[a] Department of Neurology, University of California San Francisco, United States
[b] Neurology Service, San Francisco Veterans Affairs Health Care System, United States
[c] Parkinson's Disease Research Unit, Department of Neurobiology, Barrow Neurological Institute, Phoenix, AZ, 85013, United States

ARTICLE INFO

Keywords:
Excitatory amino acid transporter 3
Parkinson's disease
Gene-Environment interaction
Glutathione
SLC1A1

ABSTRACT

Oxidative stress and α-synuclein aggregation both drive neurodegeneration in Parkinson's disease, and the protein kinase c-Abl provides a potential amplifying link between these pathogenic factors. Suppressing interactions between these factors may thus be a viable therapeutic approach for this disorder. To evaluate this possibility, pre-formed α-synuclein fibrils (PFFs) were used to induce α-synuclein aggregation in neuronal cultures. Exposure to PFFs induced oxidative stress and c-Abl activation in wild-type neurons. By contrast, α-synuclein - deficient neurons, which cannot form α-synuclein aggregates, failed to exhibit either oxidative stress or c-Abl activation. N-acetyl cysteine, a thiol repletion agent that supports neuronal glutathione metabolism, suppressed the PFF - induced redox stress and c-Abl activation in the wild-type neurons, and likewise suppressed α-synuclein aggregation. Parallel findings were observed in mouse brain: PFF-induced α-synuclein aggregation in the substantia nigra was associated with redox stress, c-Abl activation, and dopaminergic neuronal loss, along with microglial activation and motor impairment, all of which were attenuated with oral N-acetyl cysteine. Similar results were obtained using AAV-mediated α-synuclein overexpression as an alternative means of driving α-synuclein aggregation *in vivo*. These findings show that α-synuclein aggregates induce c-Abl activation by a redox stress mechanism. c-Abl activation in turn promotes α-synuclein aggregation, in a feed-forward interaction. The capacity of N-acetyl cysteine to interrupt this interaction adds mechanistic support its consideration as a therapeutic in Parkinson's disease.

1. Introduction

Identified risks for Parkinson's disease (PD) include exposure to toxins and other environmental agents that affect cell redox state, such as MPTP, rotenone, paraquat, and others (Langston et al., 1983; Sherer et al., 2003; Tanner et al., 2011). Risk for PD is also increased by genetic variants that promote formation of α-synuclein aggregates (Billingsley et al., 2018). These environmental and genetic risk factors interact, as redox state influences α-synuclein aggregation (Norris and Giasson, 2005; Scudamore and Ciossek, 2018; Sherer et al., 2003) and, conversely, α-synuclein aggregates induce oxidative stress (Deas et al., 2016; Musgrove et al., 2019). These bidirectional interactions suggest convergent or feed-forward processes that could be targeted to suppress disease progression; however, the underlying mechanisms by which these factors interact are not well characterized.

The tyrosine kinase c-Abl provides a link between cell redox state and α-synuclein aggregation in PD (Brahmachari et al., 2017). c-Abl is a ubiquitous non-receptor protein kinase that normally functions as part of the cellular DNA damage response (Maiani et al., 2011) and other processes (Sirvent et al., 2008). c-Abl in the cell cytosol can also be activated directly by oxidative stress (Sun et al., 2000). In animal models of PD, c-Abl activation promotes both α-synuclein aggregate formation and neuronal death (Brahmachari et al., 2016, 2017). The effect of c-Abl on aggregate formation is mediated in part by its phosphorylation

Abbreviations: c-Abl, cellular homolog of the v-Abl oncogene of the Abelson murine leukemia virus; EAAT3, excitatory amino acid transporter 3; HNE, hydroxynonenal; MAP, microtubule-associated protein; NAC, N-acetyl cysteine; PD, Parkinson's disease; PFF, pre-formed α-synuclein fibrils; PVDF, polyvinylidene fluoride; rAAV, recombinant adeno-associated virus; SDS, sodium dodecyl sulfate; TH, tyrosine hydroxylase

* Corresponding author at: (127) Neurology, SFVAMC, 4150 Clement St., San Francisco, CA, 94121, United States.
E-mail address: raymond.swanson@ucsf.edu (R.A. Swanson).

https://doi.org/10.1016/j.pneurobio.2021.102070
Received 21 February 2020; Received in revised form 21 January 2021; Accepted 27 April 2021

of the ubiquitin ligase parkin, which renders parkin unable to ubiquitinate α-synuclein and thus slows α-synuclein proteolysis (Imam et al., 2011; Ko et al., 2010). c-Abl also promotes aggregate formation through direct phosphorylation of α-synuclein at its tyrosine 39 residue (Brahmachari et al., 2016; Mahul-Mellier et al., 2014), and by slowing the rate of autophagic protein clearance (Karim et al., 2020). Pharmacological inhibition of c-Abl can slow disease progression in animal models of PD (Brahmachari et al., 2017; Hebron et al., 2013; Karim et al., 2020; Lee et al., 2018). Two recent clinical trials of the c-Abl inhibitor nilotinib in PD produced mixed results, but these trials were not powered to test efficacy (Pagan et al., 2020; Simuni et al., 2020). However, nilotinib has limited penetration into brain (Simuni et al., 2020) and c-Abl inhibitors as a class exhibit significant cardiac, gastrointestinal and other toxicities that could restrict its clinical use PD (Pinilla-Ibarz et al., 2015). Alternative means of suppressing c-Abl activation in PD may thus be of value.

Here we sought to determine whether c-Abl activation mediates interactions between redox stress and α-synuclein aggregate formation, and whether suppressing redox stress can suppress the effects of c-Abl on α-synuclein aggregation. We used cell culture and two mouse models of PD; stereotactic injection of pre-formed α-synuclein fibrils, and AAV-mediated α-synuclein overexpression. Our findings show that α-synuclein aggregates activate c-Abl through an oxidant stress mechanism, and that this can be blocked by the thiol repletion agent N-acetyl cysteine (NAC). Perhaps surprisingly, NAC also suppressed formation of α-synuclein aggregates. The results identify a feed-forward interaction between oxidant stress and α-synuclein aggregation and support accumulating evidence that N-acetyl cysteine could be an effective therapeutic intervention for PD.

2. Materials and methods

All studies were performed in accordance with the US PHS Policy on Humane Care and Use of Laboratory Animals and with protocols approved by the San Francisco Veterans Affairs Medical Center animal studies committee. Cell culture reagents were obtained from Sigma-Aldrich except where noted. The primary antibodies and concentrations used for western blotting (WB) and immunocytochemistry (IHC) are as follows: c-Abl, Abcam-ab15130 (WB 1:2000); phospho c-Abl 245, Cell Signaling-2861 (WB 1:1000, IHC 1:250); α-synuclein, BD Biosciences 610787 (WB 1:1000); phospho synuclein 39, BioLegend A15119B (WB 1:500, IHC 1:200); phospho synuclein 129, Abcam-ab59264 (IHC 1:1000) and Abcam-ab184674 (IHC 1:500); Parkin, Cell Signaling-2132 (WB 1:1000); 4-hydroxynonenal, Alpha Diagnostics 13-M (IHC 1:1000) and 12-S (IHC 1:2500); microtubule associated protein 2, Millipore MAB3418 (IHC 1:2000); tyrosine hydroxylase, Millipore AB1542 (IHC 1:2000); β-actin, ThermoFisher MA1−140 (WB 1:5000); Iba-1, Wako Chemicals #49874814285584 (IHC 1:500).

2.1. Pre-formed α-synuclein fibrils (PFFs)

Pre-formed human α-synuclein fibrils were prepared from recombinant human α-synuclein as described (Volpicelli-Daley et al., 2014) and stored at −80 °C. Aliquots were thawed and sonicated for 5 min immediately before use.

2.2. rAAV production

Recombinant AAV genomes were generated by inserting full length human synuclein or mCherry behind the CAG (CBA/CMV hybrid) promoter and packaged in rAAV2/9 as described (Sandoval et al., 2019). In brief, 293 T cells were transfected with genome and helper plasmids. Three days later, virus was harvested from media and cells and purified using an idodixanol gradient. Virus was quantified using digital droplet PCR, and titers were diluted to 1.0×10^{13} vector genomes / ml.

2.3. Cell culture studies

Neurons were isolated from cortices C57BL/6 wildtype or α-synuclein$^{-/-}$ mice (Jackson Labs) of both sexes on embryonic day 17–18 and plated onto poly-D-lysine coated glass coverslips as described (Brennan et al., 2009). The cultures were maintained in medium containing 5 mM glucose, with Neurobasal (Life technologies #2103049), and B27 (Life technologies #17504044) supplements, in a 5% CO_2, 37 °C incubator. Exposure to PFFs was performed by adding 1 μg / ml to culture media of neurons on day 7 *in vitro*. Where used, NAC was added on day 9 *in vitro* at a 400 μM concentration. Immunostaining and live-cell assessment of reactive oxygen species with dihydroethidium were performed as described (Brennan et al., 2009). Three to five photos were taken of each coverslip by an observer blinded to the experimental conditions, and with identical camera settings maintained within each experiment. Fluorescence intensity was measured as arbitrary units and normalized to either the number of cells or neuronal area in each field. For live-cell assessment of reactive oxygen species, 10 μM dihydroethidium (Life Technologies, D11347) was added to the culture medium 30 min prior to fixation.

Cells were lysed in Phospho-Sure lysis buffer and the tissue lysate was then sonicated on ice, agitated on a rotator at 4 °C for 1 h, and centrifuged for 30 min at 4 °C, 10,000 *g*. Proteins in the supernatant were separated by electrophoresis and transferred to PVDF membranes. The membranes were then blocked with 5% non-fat milk or goat serum, incubated with primary antibody overnight, with secondary antibody (IR 600/800 CW, Licor, #C70908−04 or #C70620−05) for 1 h, and imaged on an Odyssey gel scanner. Where chemiluminescence imaging was used, membranes were incubated with secondary antibodies (Sigma, Rabbit-GENA934 and Mouse-GENA931) and treated with Pierce Super signal reagent (ThermoFisher #34,580). For immunoblots of α-synuclein oligomers (Sasaki et al., 2015),1% SDS was added to the cell lysates, the lysates were centrifuged at 16,000 *g*, and the PVDF membranes were treated with paraformaldehyde prior to immunoblotting (Sasaki et al., 2015).

2.4. Mouse studies

The *in vivo* studies used either wild-type C57BL/6 mice or EAAC1$^{-/-}$ male mice (Aoyama et al., 2006) on the C57BL/6 background. Mice were arbitrarily assigned to treatment groups at age 9 months and euthanized at age 15 months. Where used, NAC was provided in drinking water at a concentration of 3 mg / ml and exchanged twice weekly with fresh solution, as described (Berman et al., 2011). NAC administered in this way has been shown to normalize glutathione levels in glutathione-depleted mouse brain neurons (Berman et al., 2011; Reyes et al., 2016). Of the 26 mice used for the studies there were two premature mortalities, both in the AAV-synuclein group.

2.5. Stereotactic injections

For AAV injections, a microinjection syringe was inserted to target the substantia nigra pars compacta unilaterally (anterior–posterior, +/- 3.0, medio-lateral, + 1.5, dorso-ventral, - 4.6 from bregma). 5 μl of AAV2/9 encoding either human α-synuclein or mCherry was injected at a concentration of 1.0×10^{13} vector genomes / ml), at a flowrate of 0.25 μL / minute (Benskey et al., 2018). Post-surgical incisional pain was treated with bupivacaine and buprenorphine. Stereotactic PFF injections were performed in the same way but were bilateral. Each injection delivered 10 μL of 5 μg / μl PFF or, for controls, 10 μL of PBS.

2.6. Behavioral assessments

The rota-rod test and pole tests were performed as described (Berman et al., 2011; Shiotsuki et al., 2010), with minor modifications.

Two persons handled the mice, and both were blinded to the treatment group assignments. For the rota-rod test, mice were first habituated to the task by placement for 90 s on a horizontal rod (San Diego Instruments Rota-rod) rotating at 4 rpm (1st day) and 5.5 rpm (2nd day), 5 times each day. For testing, mice were placed on the horizontal rod at a start speed 0 rpm and an acceleration rate of 6 rpm / minute, and the time until fall from the rod was recorded. Tests were repeated 6 times each day for 2 consecutive days. The outlier (lowest value) for each mouse was discarded and the average time from the remaining 11 trials was recorded for each mouse. For the pole test, mice were placed face-up at the top of a pole (45 cm length, 1.2 cm diameter), wrapped in tape for grip. A piece of cardboard was fitted over the top of the pole so that the mouse had to turn face down to descend the pole. Each assessment involved 2 days of habituation followed by 3 days of testing. An experimenter guided the mouse to complete the task during habituation. Testing was performed twice a day for three consecutive days and video was recorded. The recordings were later analyzed by an observer who was also blinded to the treatment conditions and scored for turn-around time (time taken to face downward) and descent time (time taken to come down the pole). However, descent-time was not used for data analysis because some impaired mice were unable to descend the pole normally and instead either slid down or used their tails to assist. Timing was begun with the first mouse movement, and any time exceeding 3 s during which the mouse was motionless was subtracted from the total time. Times were averaged for each mouse over the 3 trials.

2.7. Brain harvest and tissue preparation

Mice were transcardially perfused with 200 mL of 0.9 % cold saline and brains were removed. The brains were bisected sagittally. The right half was immersed in 4% paraformaldehyde in phosphate-buffer (PB) for 48 h, followed by immersion in 20 % sucrose for 48 h, and sectioned in a cryostat (40 μm thickness). The left halves of the bisected brains were stored at -80 °C until use for immunoblot preparation. At that time, a 1.0 mm coronal section was isolated from the frozen hemi-brain at the level of the substantia nigra and homogenized in PhosphoSure lysis buffer containing Hank's phosphatase and protease inhibitor cocktail (ThermoScientific #78,430). The tissue lysate was then sonicated on ice, and treated as described for the cell culture studies.

For immunoprecipitation assays, mid-brain lysates obtained in PhosphoSure lysis buffer were incubated with protein I/G magnetic beads (Sigma-Aldrich)coated with anti-phosphotyrosine antibody (4G10, EMD Millipore) and incubated for 2 h at 4 °C. The beads were then washed, and bound proteins eluted with SDS-sample buffer. Parkin levels in the recovered immune complexes were quantified as described (Ghosh and Geahlen, 2015)

2.8. Immunohistochemistry

Sections were rinsed in PBS, then incubated in blocking buffer (10 % goat serum and 0.1 % Triton X-100 in 0.1 M PB) for 1 h at room temperature. The sections were then incubated with designated primary antibodies overnight in blocking buffer. After washing, the sections were incubated with secondary antibodies that were either biotinylated or coupled to fluorescent tags. Biotinylated IgG secondary antibody was used at 5 μg / ml (Invitrogen, Carlsbad, CA) for 2 -h incubations, then processed using a Vector ABC kit (Vector laboratories). The horseradish peroxidase reaction was detected with diaminobenzidine and H_2O_2. Alexa Fluor secondary antibodies were used at 1:2000 dilutions for 2 -h incubations. After washing, the sections were mounted on slides with permount for DAB stained sections, or with ProLong™ Gold Antifade Mountant with or without DAPI (ThermoScientific, P36931, P36930) for fluorescent antibodies. Image analysis was done by an experimenter blinded to the experimental groups. Three to five photos were taken of the region of interest on each section. Identical camera settings were maintained for image capture within each experiment. In most studies fluorescence intensity was measured as arbitrary units and normalized to either the number of cells or TH-positive cells in each field. Where noted, neuronal cytoplasm as identified by either MAP2 or TH staining to define the regions of interest in which the 4HNE, phospho-Abl, or phospho syn129 signals were analyzed. In the studies using AAV, signals from the midbrain were normalized to signal from (non-transfected) cerebral cortex. Iba-1 expression was measured as ((Iba-1 optical density) – (background optical density)) X (Iba-1 area), where optical density was measured in arbitrary units, area was measured in pixels / photomicrograph, and background optical density was measured in pixels clearly devoid of microglial processes.

For glutathione immunohistochemistry, 40 μm thick sections were incubated with 10 mM N-ethyl maleimide for 4 h at 4 °C, washed, and incubated with mouse anti-glutathione-NEM (clone 8.1GSH, Millipore) as previously described and calibrated (Won et al., 2015). After washing, the sections were incubated with Alexa Fluor 488-conjugated goat anti-mouse IgG (1:1000; Thermo Fisher Scientific) for 1 h. Data from each animal were normalized to signal from cerebral cortex.

A stereological approach was used to assess tyrosine hydroxylase (TH) - positive neurons in the substantia nigra pars compacta. Three coronal sections were analyzed from each mouse, taken at the levels of -2.6, -3.2, and -3.6 mm anterior to Bregma, which nearly span the pars compacta (Fu et al., 2012). TH - positive cell bodies were counted in the substantia nigra pars compacta as defined (Fu et al., 2012) in each brain hemisection. The cell counts were made by an observer blinded to experimental conditions, and the counts for each mouse were expressed as the average number of cells per hemisection.

2.9. Statistical analyses

For cell culture data, the "n" was defined as the number of experiments done using independent culture preparations, each with 3–4 internal replicates. For mouse studies, "n" denotes the number of animals in each group. Where two groups were compared, data were analyzed by the 2- sided student's *t*-test or Mann-Whitney test. For analyzing three or more groups, we used one-way ANOVA followed by the Bonferroni or Dunnett's test. GraphPad Prism 8.0 software was used for the statistical analyses.

3. Results

Mouse neuron cultures were used to establish the causal relationships between α-synuclein aggregates, oxidant stress, and c-Abl activation. Neurons were incubated with PFFs for 7–10 days to induce aggregation of endogenous α-synuclein (Volpicelli-Daley et al., 2014). Aggregate formation was confirmed by western blotting for α-synuclein oligomers, and by immunostaining for phospho-129 α-synuclein (Fig. 1A-C). Aggregate formation was accompanied by oxidative stress, as shown by formation of the lipid peroxidation product 4-hydroxynonenal (Fig. 1C,D). Neurons incubated with PFFs also showed a large increase in activated c-Abl, with no change in total c-Abl (Fig. 1D). By contrast, neurons cultured from α-synuclein $^{-/-}$ mice did not show phospho-129 α-synuclein immunoreactivity, confirming specificity of the signal under these experimental conditions (Fig. 2A). α-synuclein$^{-/-}$ neurons incubated with PFFs also failed to exhibit the increased c-Abl activation (phosphorylation) or 4-hydroxynonenal formation observed in wild-type neurons (Fig. 2B,C), indicating a requisite role for the endogenously formed α-synuclein aggregates in these processes. c-Abl activation in the PFF-exposed cells was further evidenced by a large increase in phospho-39 α-synuclein (Suppl Fig. 1A,B), which is produced by activated c-Abl (Mahul-Mellier et al., 2014). Together, these results show that PFF-induced aggregation of endogenous

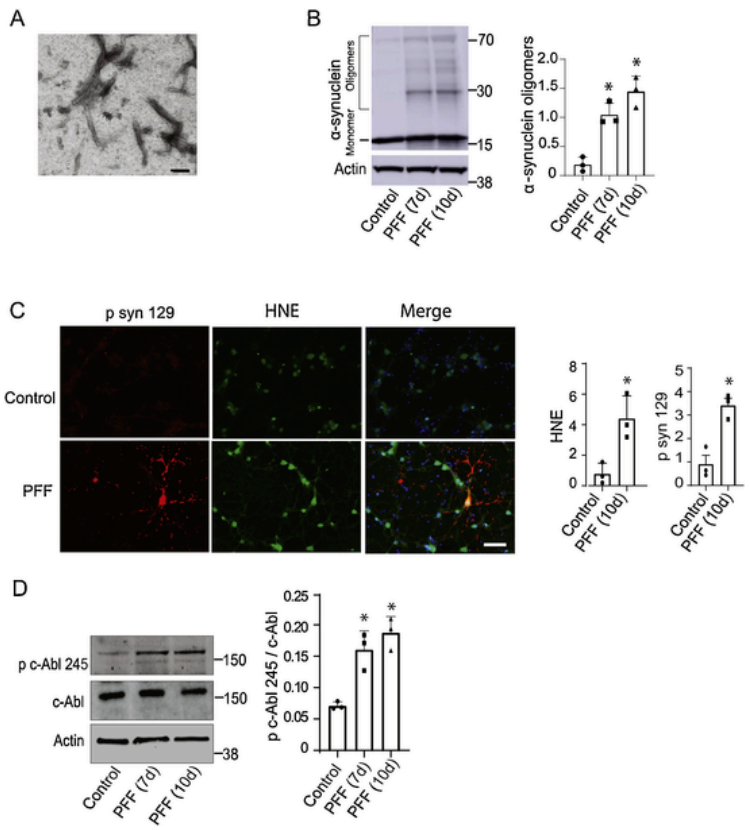

Fig. 1. Pre-formed α-synuclein fibrils induce α-synuclein aggregation, oxidative stress, and c-Abl activation in cultured neurons. **(A)** Human α-synuclein pre-formed fibrils (PFFs) visualized by electron microscopy. Scale bar = 200 nm **(B)** Western blot showing formation of α-synuclein oligomers in primary cortical neurons treated with PFFs (5 μg / ml) for 7 or 10 days. Oligomers were quantified by summing the band densities over the molecular weight range indicated by bracket (20 - 75 Kda) and normalized to the corresponding actin loading control. n = 3, *p < 0.01 vs. control by ANOVA and Dunnett's test. **(C)** Immunostaining of primary cortical neurons treated with human PFFs for 10 days. α-synuclein aggregates are identified by p syn 129 (α-synuclein phosphorylated at serine 129; red), oxidative stress is identified by the lipid oxidation marker HNE (4-hydroxynonenal; green), and cell nuclei are identified by DAPI (blue). Scale bar = 10 μm. The immunostaining is quantified with fluorescence expressed in arbitrary units and normalized to the number of cell nuclei in each field, n = 3, *p < 0.01 by Student's *t*-test. **(E)** Western blot shows c-Abl activation (c-Abl phosphorylation at tyrosine 245) in neurons treated with PFFs for 7 or 10 days. Quantification shows ratio of the phospho c-Abl band to total c-Abl. n = 3, *p < 0.01 vs. control by ANOVA and Dunnett's test.

α-synuclein leads to both oxidative stress and c-Abl activation in the cultured neurons.

3.1. Oxidative stress alone is sufficient to activate c-Abl in culture and in vivo

To determine whether oxidative stress *per se* is sufficient to cause c-Abl activation in neurons, we evaluated cultures after exposure to hydrogen peroxide. Western blots prepared from these cultures showed a robust increase in c-Abl activation (Fig. 3A). The H_2O_2 - induced c-Abl activation was suppressed by NAC, a thiol agent previously shown to support neuronal glutathione synthesis (Berman et al., 2011; Reyes et al., 2016) and to have salutary effects in animal models of PD (Berman et al., 2011; Clark et al., 2010; Sharma et al., 2007). We next evaluated the effect of redox stress on c-Abl activation *in vivo*, using EAAC1$^{-/-}$ mice. EAAC1 (also termed EAAT3 and SLC1A1) is a neuronal cysteine transporter, and mice deficient in EAAC1$^{-/-}$ mice exhibitexhibit diminished neuronal glutathione levels and chronic neuronal oxidative stress (Aoyama et al., 2006; Berman et al., 2011), as demonstrated in Fig. 3B. Western blot and immunofluorescence measures of phospho c-Abl in EAAC1$^{-/-}$ mouse midbrain showed increased c-Abl activation relative to Wt mice. The increase c-Abl activation observed in the EAAC1$^{-/-}$ brain was attenuated by 10 days' treatment with NAC administered as 3 mg / ml in drinking water (Fig. 3C,D), thus demonstrating that oxidative stress is sufficient to drive neuronal c-Abl activation *in vivo*.

3.2. N-acetyl cysteine suppresses oxidant stress and c-Abl activation in cultured neurons

Given that PFF-induced α-synuclein aggregates generate oxidative stress, and oxidative stress is sufficient to drive c-Abl activation, we next tested whether suppressing oxidative stress with NAC could prevent c-Abl activation in PFF-exposed neurons. We found that NAC added to the cell culture medium effectively suppressed PFF-induced oxidative stress, as evidenced both by decreased formation of HNE and decreased oxidation of dihydroethidium (Fig. 4A,B). NAC likewise suppressed c-Abl activation as demonstrated by immunostaining and western blots (Fig. 4C,D). The effect of NAC on c-Abl activation was comparable to that achieved by the c-Abl inhibitor nilotinib, which is a targeted inhibitor of c-Abl (Weisberg et al., 2006) and included here as a positive control. Importantly, both NAC and nilotininb also decreased p syn 129 formation in the PFF-exposed neurons (Fig. 4E).

3.3. PFF injections induce oxidative stress and c-Abl activation in vivo

We next evaluated effects of PFF-induced oxidative stress and c-Abl activation in mouse brain. Mice aged 9–10 months received bilateral injections of PFFs (or saline control) into the substantia nigra (Thakur et al., 2017). NAC was added to the drinking water of half of the PFF-injected mice beginning 2 weeks after the injections and continued until brain harvest 6 months later. Assessment of the substantia nigra in the brains of these mice showed that PFF injections decreased neuronal glu-

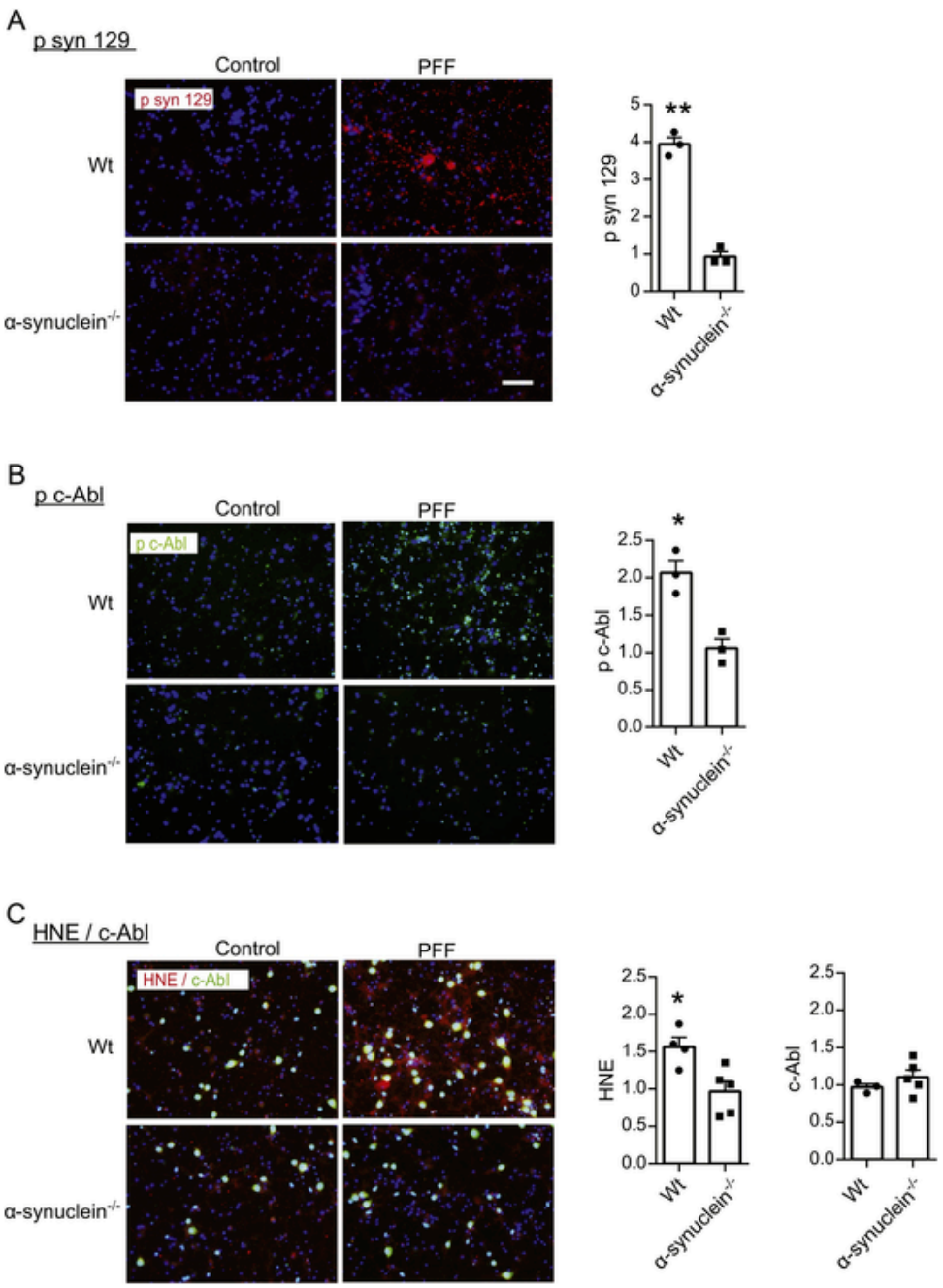

Fig. 2. Lack of PFF effects on α-synuclein $^{-/-}$ neurons. Cortical neurons from Wt and α-synuclein$^{-/-}$ mice were incubated with PFFs for 14 days and immunostained in parallel for (A) p syn 129 (red); (B) p c-Abl 245 (green); (C) total c-Abl (green) and (C) HNE (red). Nuclei were counterstained blue with DAPI. Scale bar = 20 μM. Quantified data from each experiment (n = 3 - 4) are normalized to number of cell nuclei and expressed relative to values measured in the α-synuclein$^{-/-}$ cells in each experiment. **p < 0.01, *p < 0.05 by Student's *t*-test.

tathione content, which can be both a cause and an effect of oxidative stress. This decrease was attenuated in the mice treated with NAC (Fig. 5A). PFF injections also produced α-synuclein aggregation and lipid peroxidation in substantia nigra neurons (Fig. 5B). The aggregates and lipid peroxidation were prominent in dopaminergic (tyrosine hydroxylase - positive) neurons, but not restricted to these cells. PFF-injected mice treated with NAC exhibited a substantial reduction in lipid peroxidation (Fig. 5B). Mice treated with NAC also showed suppression of c-Abl activation, as assessed by measures of c-Abl phosphorylation (Fig. 5C), phospho-synuclein 39 formation, and Parkin phosphorylation (Suppl. Fig. 1C, D), thus supporting redox stress as the primary factor driving c-Abl activation in the PFF-injected brains. There was also a substantial reduction in α-synuclein aggregate formation in the mice treated with NAC (Fig. 5B) similar to that observed in the cell culture studies (Fig. 4E).

Evaluation of dopaminergic (TH - positive) neurons in the substantia nigra pars compacta showed a loss in mice subjected to PFF injections, and this loss was attenuated in mice treated with NAC (Fig. 6A). The loss of TH neurons in the substantia nigra pars compacta was accompanied by microglial hypertrophy and increased Iba-1 expression (Fig. 6B). The PFF-injected mice also exhibited impaired performance on the rota-rod test and pole tests, and these motor deficits were likewise mitigated in the mice treated with NAC.

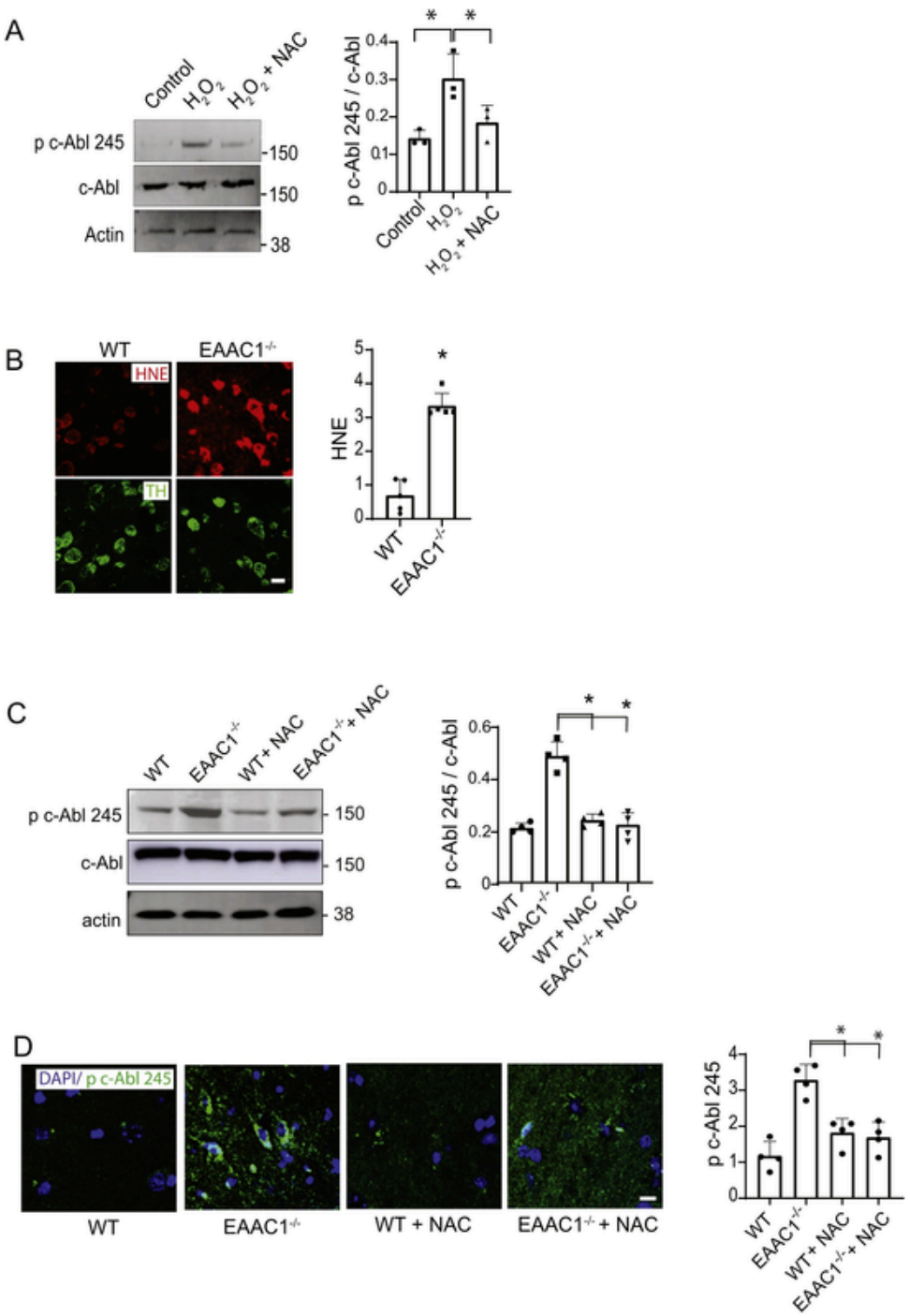

Fig. 3. Oxidative stress alone is sufficient to activate c-Abl in culture and *in vivo*. **(A)** Western blot shows activation (phosphorylation) of c-Abl in neurons treated with 100 μM hydrogen peroxide for 30 min, and reduced activation in the additional presence of 500 μM N-acetyl cystine (NAC). Quantification shows ratio of the phospho c-Abl band to total c-Abl. n = 3, *p < 0.01 by ANOVA and the Bonferroni test. **(B)** Oxidative stress in tyrosine hydroxylase expressing (TH, green) neurons of wild-type (Wt) and EAAC1$^{-/-}$ mouse midbrain, as detected by formation of 4-hydroxynonenal (HNE, red). Scale bar =10 μm. n = 3, * p < 0.01 by Student's *t*-test. **(C)** Western blot showing activation (phosphorylation) of c-Abl in midbrain of EAAC1$^{-/-}$ mice and suppression of this activation in EAAC1$^{-/-}$ mice treated with NAC for 10 days. Quantification shows ratio of phospho c-Abl band to total c-Abl, n = 3; *p < 0.01 by ANOVA and the Bonferroni test. **(D)** Immunostaining showing increased phospho c-Abl (green) in midbrain of EAAC1$^{-/-}$ mice and reversal of this increase in EAAC1$^{-/-}$ mice treated with NAC for 10 days. Cell nuclei are labeled with DAPI. Scale bar =10 μm. n = 3-4, *p < 0.01 by ANOVA and the Bonferroni test.

3.4. AAV-mediated α-synuclein overexpression induces oxidative stress and c-Abl activation

As a second mouse model of α-synuclein aggregate formation, we injected adeno-associated virus expressing human α-synuclein into the substantia nigra (Ip et al., 2017). Controls were injected with AAV expressing mCherry (Fig. 7A). NAC was added to the drinking water of half of the mice beginning 2 weeks after the AAV injections and continued until brain harvest 6 months later. Assessment of the substantia nigra in these brains showed that the AAV α-synuclein injections produced α-synuclein aggregates and oxidative stress, along with c-Abl activation (Fig. 7, C). Co-labeling for TH revealed phospho (activated) c-

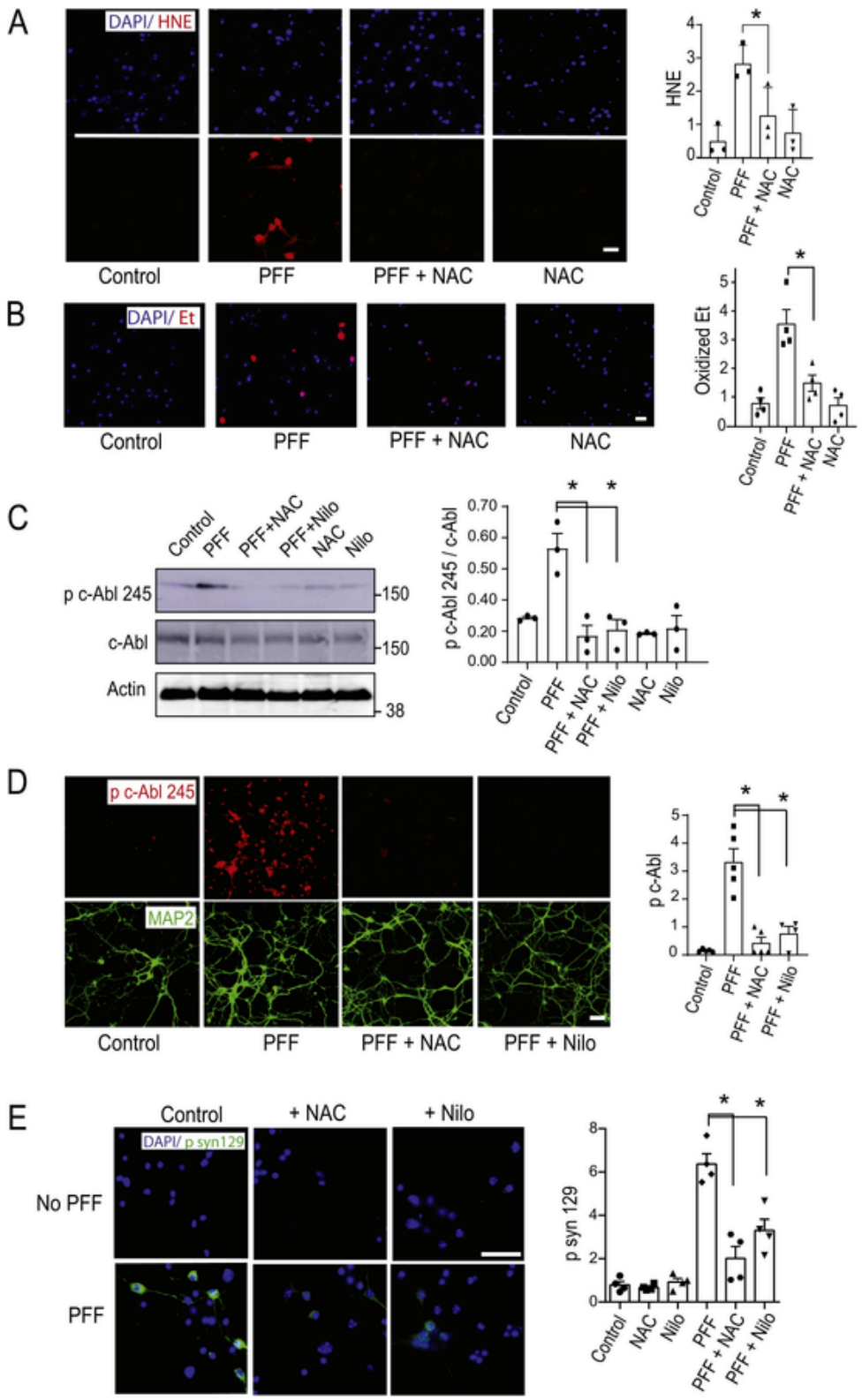

Fig. 4. N-acetyl cysteine suppresses oxidant stress and c-Abl activation in neuron cultures. (**A**) Oxidant stress detected by formation of 4-hydroxynonenal (HNE, red) in neurons incubated with PFFs for 10 days with or without 500 μM N-acetyl cysteine (NAC). Cell nuclei are labeled blue with DAPI. Scale bar = 10 μm. Quantified HNE signal is expressed in arbitrary units and normalized to the number of cell nuclei in each field. n = 3, * $p < 0.01$ by ANOVA and the Bonferroni test. (**B**) Oxidant stress detected by formation of oxidized fluorescent ethidium species (Et, red) in neurons incubated with PFFs for 10 days with or without 400 4μM NAC. Cell nuclei are stained blue with DAPI. Scale bar = 20 μm. Quantified Et signal is expressed in arbitrary units and normalized to the number of cell nuclei in each field. n = 4, * $p < 0.01$ by ANOVA and the Bonferroni test. (**C**) Western blot shows activation (phosphorylation) of c-Abl in neurons treated 10 days with PFFs, and reduced activation in the additional presence of 500 μM NAC or 10 μM nilotinib (Nilo). Quantification shows ratios of the phospho c-Abl bands to total c-Abl, n = 3,

◀ *p < 0.01 by ANOVA and the Bonferroni test. (**D**) Immunostaining shows c-Abl activation (c-Abl phosphorylation at tyrosine 245; red) in neurons treated 10 days with PFFs, and reduced activation in the additional presence of 400 μM NAC or 10 μM nilotinib. MAP2 (green) identifies neuronal cytoplasm. Scale bar =20 μm. Graph shows p c-Abl 245 fluorescence expressed in arbitrary units and normalized to the neuronal (MAP2) area in each field, n = 4, *p < 0.01 by ANOVA and the Bonferroni test. (**E**) α-synuclein aggregation as detected by p syn 129 immunostaining (green) in neurons incubated with PFFs for 10 days with or without addition of 500 μM N-acetyl cysteine (NAC) or 10 μM nilotinib. Scale bar =20 μm. Quantified p syn 129 signal is expressed in arbitrary units and normalized to the number of cell nuclei in each field. n = 3, * p < 0.01 by ANOVA and the Bonferroni test.

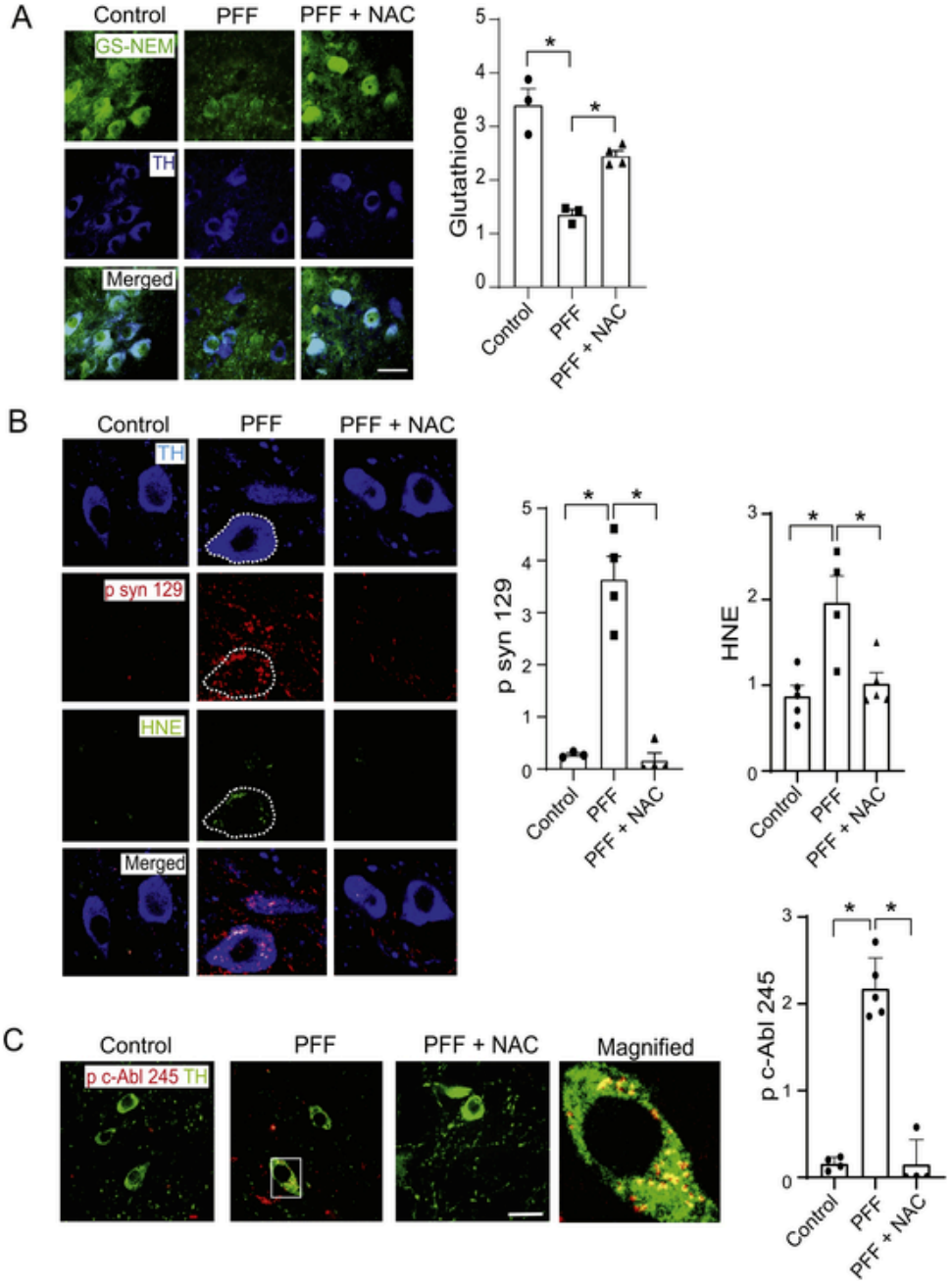

Fig. 5. PFFs induce oxidative stress and c-Abl activation *in vivo*. (**A**) Immunostaining for glutathione (GS-NEM, green) in TH - positive (blue) cells of the substantia nigra. Brains were harvested 6 months after PFF injections. Where indicated, the mice also received 3 mg/mL NAC in drinking water beginning 2 weeks post-injection. Scale bar =10 μm. Quantified data are from n = 3 - 4 mice; *p < 0.05 by ANOVA and the Bonferroni test. **(B)** Immunostaining at the injection site identifying dopaminergic cell bodies (TH; blue), α-synuclein aggregates (p syn 129; red), and lipid peroxidation (HNE; green). Dotted line exemplifies area defined by a TH-positive neuron for quantification of p syn 129 and HNE. p syn 129 and HNE fluorescence are expressed as arbitrary units / TH-positive pixel. n = 3 - 4, *p < 0.01 by ANOVA and the Bonferroni test. **(C)** Immunostaining for activated c-Abl (p c-Abl 245; red) in TH - positive (green) cells. White rectangle denotes field shown in magnified view. Quantified data shows phospho c-Abl signal fluorescence within TH - positive cells. n = 3-4; *p < 0.01 by ANOVA and the Bonferroni test.

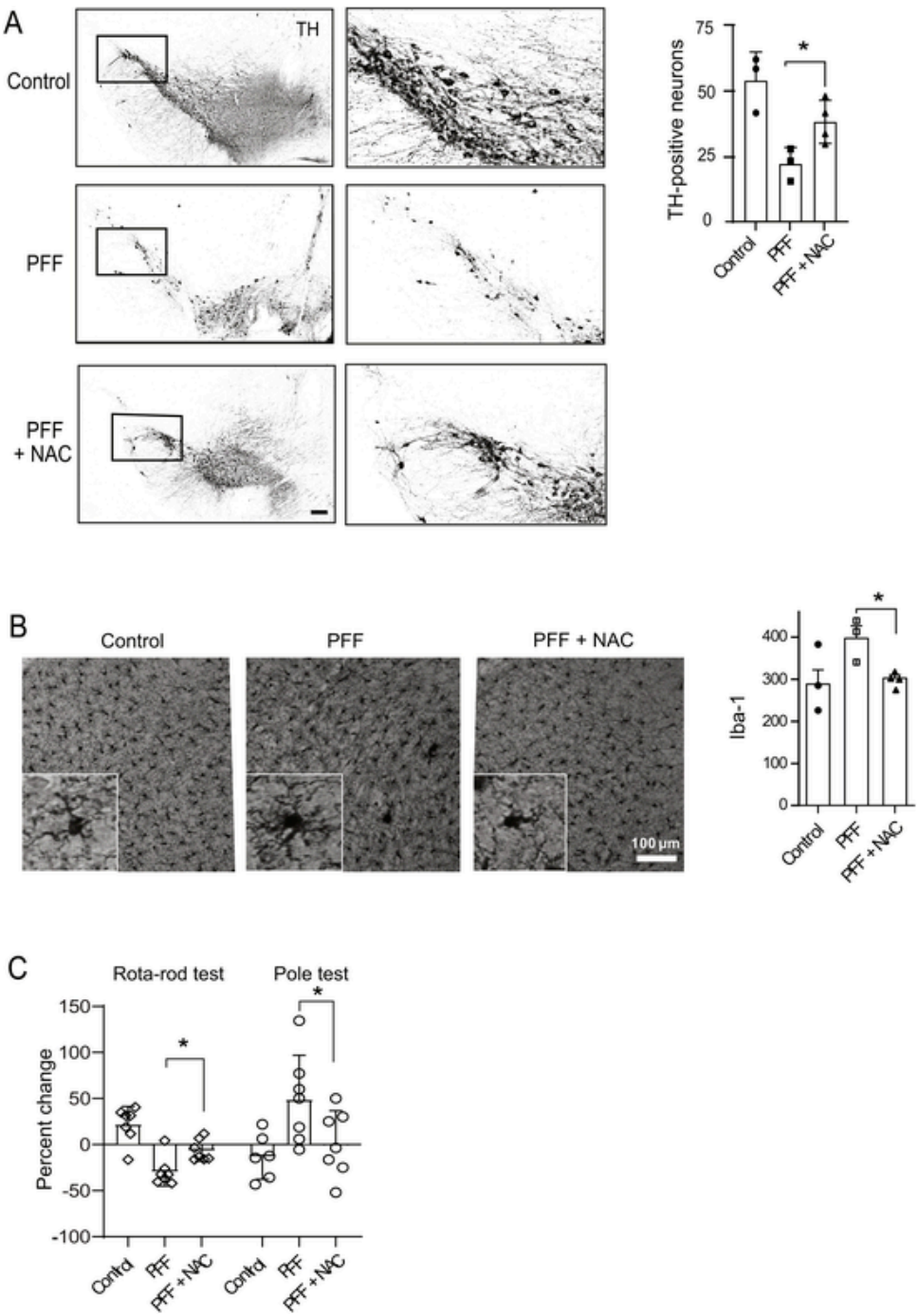

Fig. 6. Effects of NAC in PFF-injected mice. **(A)** TH-positive cells in substantia nigra of control mice, PFF-injected mice, and PFF-injected mice treated with NAC. Scale bar =50 µm. Rectangles denote areas of magnified views (right column). Graph shows mean number of TH-positive neurons per hemisection. n = 3 - 4; *p < 0.01 by ANOVA and the Bonferroni test. **(B)** Immunostaining for Iba-1 in substantia nigra shows hypertrophy and increased Iba-1 expression in microglia. Scale bar = 100 µM. Graph shows integrated Iba-1 signal densities; n = 3 - 4; *p < 0.05 by ANOVA and the Bonferroni test. (**C**) Performance on rota-rod and pole tests 4 months after injections. Data for each mouse are normalized to baseline performance. n = 6 - 8; *p < 0.01 by ANOVA and the Bonferroni test. Mean baseline time on the rota-rod was 103 s, and mean baseline turn-around time on the pole test was 2.1 s.

Abl in dopaminergic neurons (Fig. 7C). Dopaminergic cell loss could not be assessed in the substantia nigra of these mice because of insufficient material for stereological assessment. However, immunostaining for dopaminergic projections into the striatum showed a decrease in TH - positive innervation in brains injected with AAV-α-synuclein, and an attenuation of this decrease by NAC treatment (Fig. 7D). As with the PFF injections, mice injected with AAV driving overexpression of α-synuclein also exhibited impaired motor dexterity as assessed by the rota-rod test and pole test, and the deficit observed on the rota-rod test was attenuated by NAC treatment.

4. Discussion

Epidemiological studies have identified both genetic and environmental factors that increase risk for in PD. Most of the genetic factors known to increase risk for PD affect α-synuclein expression or degradation, whereas most environmental risk factors induce oxidative stress

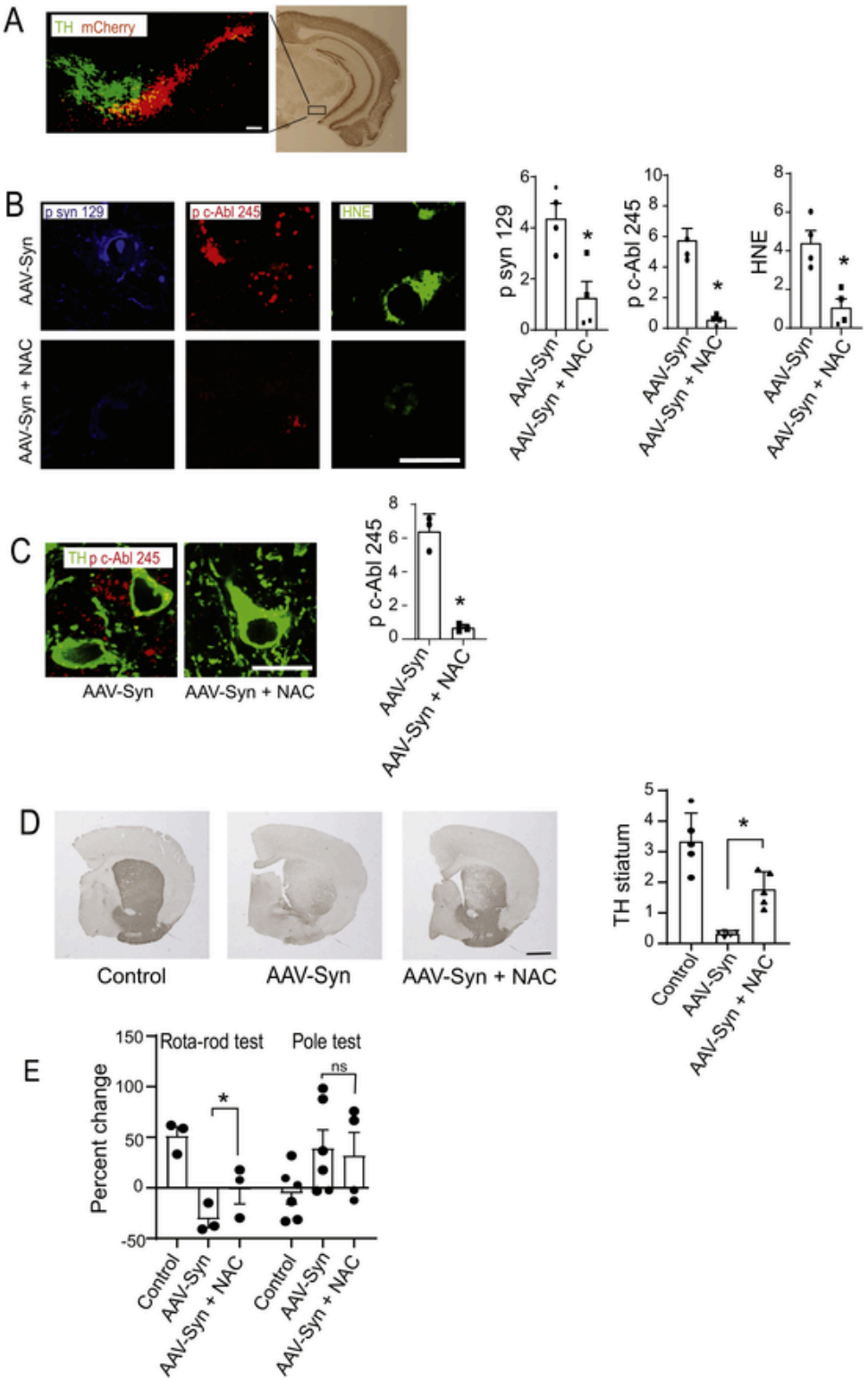

Fig. 7. NAC improves outcome after AAV-mediated α-synuclein overexpression. **(A)** Coronal hemisection showing site of AAV injection and virus expression (red; mCherry). Immunostaining for TH (green) identifies dopaminergic neurons. Scale bar =250 μm. **(B** Images taken from midbrain showing HNE (green), phospho c-Abl (red) and phospho syn 129 (blue) in mice 6 months after injection with α-synuclein AAV, with or without subsequent oral NAC treatment. Scale bar =10 μm. Quantification of midbrain HNE, c-Abl and phospho syn 129 signals are expressed relative to signal in ipsilateral cerebral cortex. n = 3 - 4; *p < 0.01 by Student's *t*-test. **(C)** p c-Abl 245 (red) in TH positive cells (green) from substantia nigra of mice injected with α-synuclein AAV with or without subsequent NAC treatment. Scale bar =10 μm Quantified results are from n = 3 - 4; *p < 0.01 0.01 by Student's *t*-test. **(D)** Immunostaining of TH in striatum of mice injected with α-synuclein AAV-syn with and without subsequent NAC treatment. Scale bar =250 μm. Quantified results are from n = 3 - 4; *p < 0.01 **(F)** Performance on rota-rod test and pole tests 5 months after AAV injections. Data for

◀ each mouse are normalized to baseline performance. n = 4 - 6; *p < 0.01 by ANOVA and the Bonferroni test. Mean baseline time on the rota-rod was 94.3 s, and mean baseline turn-around time on the pole test was 1.9 s.

(Simon et al., 2020). Interactions between α-synuclein and cell redox state may thus act as convergent mechanisms of disease progression. Here we show that α-synuclein aggregates activate c-Abl activation by a process involving redox stress, that NAC suppresses the oxidant stress caused by α-synuclein aggregates, and that this in turn suppresses both c-Abl activation and aggregate formation itself (Fig. 8).

Large, histochemically identifiable intracellular aggregates of α-synuclein (Lewy bodies) in neurons of the substantia nigra are a diagnostic feature of PD. These large aggregates are unlikely to be directly cytotoxic, but are associated with toxicity that is putatively mediated by smaller, oligomeric aggregates or by products cleaved from aggregates (Grassi et al., 2018), or by sequestration of soluble α-synuclein (Benskey et al., 2018). Here we used PFFs to induce formation of α-synuclein aggregates in neuronal cultures and *in vivo*. In the cell culture studies, PFF exposure induced oxidative stress and c-Abl activation in wild-type but not α-synuclein deficient neurons, thus confirming the role of endogenous α-synuclein in these processes. How α-synuclein aggregates lead to redox stress was not evaluated here, but prior work suggests that this may occur through the interaction of aggregates or aggregate cleavage products with mitochondria (Nakamura, 2013; Wang et al., 2019) or transition state metals in neuronal cytosol (Deas et al., 2016). Aggregates may also activate the superoxide-producing enzyme NADPH oxidase, which has been identified as a potential pathogenic factor in PD (Cristovao et al., 2012).

c-Abl contributes to pathogenesis in both cell and animal models of PD by promoting formation and slowing autophagic degradation of α-synuclein aggregates (Brahmachari et al., 2017; Karim et al., 2020). While the trigger for c-Abl activation in PD is not established, studies using non-neuronal cell types demonstrate that oxidative stress can activate c-Abl in non-neuronal cells by both direct and indirect pathways. (Brahmachari et al., 2017; Hantschel and Superti-Furga, 2004; Lawana et al., 2017; Sun et al., 2000). Our findings confirmed that oxidant stress is sufficient to induce c-Abl in neurons, as demonstrated both in cultures with acute exposure to H_2O_2, and *in vivo* using the EAAC1$^{-/-}$ mouse of chronic neuronal redox stress. Our studies additionally showed that NAC suppressed c-Abl activation in both of these settings.

Results obtained with PFF injections into mouse brain were concordant with the cell culture observations: PFFs induced α-synuclein aggregation, oxidative stress, and c-Abl activation, each of which were suppressed by chronic oral NAC administration. PFF-injected brains also showed a loss of TH-positive neurons in the substantia nigra, attenuated in mice treated with NAC. The loss of TH-positive cells was

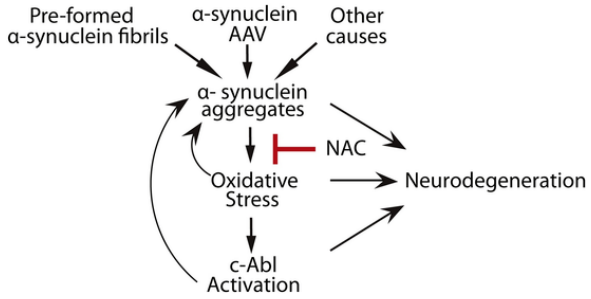

Fig. 8. Proposed Interactions between α-synuclein aggregates, oxidative stress, and c-Abl. α-synuclein aggregates produce oxidative stress, which drives c-Abl activation. Oxidative stress and c-Abl activation both contribute to α-synuclein aggregation, in a potentially feed-forward process. NAC suppresses the oxidative stress induced by α-synuclein aggregates and thereby attenuates c-Abl activation and further α-synuclein aggregation. c-Abl activation in both neurons (Karim et al., 2020; Zhou et al., 2017) and microglia (Lawana et al., 2017) may additionally contribute to neuronal demise.

accompanied by morphological hallmarks of microglial activation. Microglial activation is induced by both oxidative stress and by downstream effects of c-Abl (Lawana et al., 2017) and likely contributes to neuronal loss in PD (Bartels et al., 2020). It is thus possible that the neuroprotective effects of NAC observed in the PFF-injected mice may be mediated in part by attenuated microglial activation.

To complement the studies performed with PFFs, we also used an AAV-mediated α-synuclein overexpression approach that likewise induces aggregate formation (Gombash et al., 2013). Both approaches employed relatively old mice, age 9–15 months, which are more prone to develop α-synuclein aggregates and better mimic human PD. Results obtained in the AAV model were in agreement with those observed in the PFF model. In both models, the severity of the motor deficits was relatively modest, consistent with prior studies indicating relative preservation of motor function in mice with incomplete or unilateral injury to substantia nigra (Dauer and Przedborski, 2003).

NAC provides neurons with cysteine, the rate-limiting substrate for de-novo glutathione synthesis (Aoyama et al., 2008). Glutathione levels are selectively decreased in the substantia nigra of patients with PD (Dexter et al., 1994; Zeevalk et al., 2008), and studies using animal models suggest that this decrease contributes to disease progression (Berman et al., 2011; Chinta and Andersen, 2006; Martin and Teismann, 2009; Monti et al., 2019). Glutathione is crucial for intracellular redox homeostasis because it is used for fast, enzymatically catalyzed oxidant scavenging. Glutathione is also used for repair of oxidized proteins and for export of xenobiotic compounds and other potential toxicants. Glutathione is converted from its reduced form (GSH) to its oxidized form (GSSG) during oxidant scavenging and protein repair. GSSG is normally reduced back to GSH, but when the rate of GSSG production exceeds capacity for recycling back to GSH the excess GSSG is exported (Ballatori et al., 2009), leading to a net decrease in total cell glutathione. Systemically administered NAC has been shown to normalize neuronal glutathione levels during oxidative stress (Reyes et al., 2016; Won et al., 2015), and as demonstrated in the present study, 3 mg / ml of NAC in water was sufficient to maintain normal glutathione levels in neurons containing α-synuclein aggregates. NAC has been shown to have beneficial effects in both toxin and genetic models of PD (Berman et al., 2011; Clark et al., 2010; Monti et al., 2016; Rahimmi et al., 2015; Seaton et al., 1997; Watabe and Nakaki, 2007). Results of the present studies suggest that the salutary effects of NAC in these models may be mediated in part by suppressing c-Abl activation.

NAC can support neuronal glutathione levels at sub-micromolar cerebrospinal NAC concentrations (Reyes et al., 2016). NAC may also have additional actions on neurons mediated by its effects on cell redox state or ferroptosis (Karuppagounder et al., 2018). At far higher concentrations NAC also has a direct antioxidant effect by virtue of its reactive cysteine thiol (Rushworth and Megson, 2014; Samuni et al., 2013), and this may be its dominant mode of action in cell cultures, where cysteine sufficient for glutathione synthesis is generally available in the culture medium.

In addition to suppressing oxidant stress and c-Abl activation, NAC also decreased formation of α-synuclein aggregates. Reduced α-synuclein aggregation was also observed with nilotinib, suggesting that the effect of NAC was secondary to its effects on c-Abl activation. The effect of NAC on aggregate formation was substantial in both the cell culture and in vivo studies, rendering it difficult to establish whether the associated effects of NAC on oxidant stress and dopaminergic cell loss were direct effects or indirect effects mediated by the lessened aggregate formation. However, given the feed-forward relationships between these events (Fig. 8), a distinction between these two alternatives may not be meaningful.

4.1. Conclusions

The findings presented here support a feed-forward process whereby redox stress promotes α-synuclein aggregation via c-Abl activation, and α-synuclein aggregate formation in turn produces redox stress. We also show that this process can be interrupted by NAC. NAC is inexpensive, FDA-approved, orally absorbed, and enters human cerebrospinal fluid at biologically active concentrations (Berman et al., 2011; Reyes et al., 2016). Thiol repletion using NAC or other agents has been repeatedly cited as a promising approach for slowing PD progression (Martinez-Banaclocha, 2012; Monti et al., 2019; Reyes et al., 2016; Virel et al., 2019; Zeevalk et al., 2008), and results of the present study provide additional mechanistic support for this approach.

Author Contributions

S.G. and R.A.S contributed to the conception and design of the study; S.G., S.J.W., R. F., N.J.M.B., J.P., J.S., L.W., J.W., A.H., and F.P.M. contributed to the acquisition and analysis of data; S.G., S.J.W., and R.A.S. contributed to drafting the text and preparing the figures.

Declaration of Competing Interest

The authors report no declarations of interest.

Acknowledgements

This work was supported by the U.S. National Institutes of Health (NS105774, to R.A.S.; DK108798, to F. M.) and Dept. of Veterans Affairs (BX003249, to R.A.S.).

Appendix A. The Peer Review Overview and Supplementary data

The Peer Review Overview and Supplementary data associated with this article can be found in the online version, at doi: https://doi.org/10.1016/j.pneurobio.2021.102070

References

Aoyama, K., Suh, S.W., Hamby, A.M., Liu, J., Chan, W.Y., Chen, Y., Swanson, R. A., 2006. Neuronal glutathione deficiency and age-dependent neurodegeneration in the EAAC1 deficient mouse. Nat. Neurosci. 9, 119–126.
Aoyama, K., Watabe, M., Nakaki, T., 2008. Regulation of neuronal glutathione synthesis. J. Pharmacol. Sci. 108, 227–238.
Ballatori, N., Krance, S.M., Marchan, R., Hammond, C.L., 2009. Plasma membrane glutathione transporters and their roles in cell physiology and pathophysiology. Mol. Aspects Med. 30, 13–28.
Bartels, T., De Schepper, S., Hong, S., 2020. Microglia modulate neurodegeneration in Alzheimer's and Parkinson's diseases. Science 370, 66–69.
Benskey, M.J., Sellnow, R.C., Sandoval, I.M., Sortwell, C.E., Lipton, J.W., Manfredsson, F.P., 2018. Silencing alpha synuclein in mature nigral neurons results in rapid neuroinflammation and subsequent toxicity. Front. Mol. Neurosci. 11, 36.
Berman, A.E., Chan, W.Y., Brennan, A.M., Reyes, R.C., Adler, B.L., Suh, S.W., Kauppinen, T.M., Edling, Y., Swanson, R.A., 2011. N-acetylcysteine prevents loss of dopaminergic neurons in the EAAC1-/- mouse. Ann. Neurol. 69, 509–520.
Billingsley, K.J., Bandres-Ciga, S., Saez-Atienzar, S., Singleton, A.B., 2018. Genetic risk factors in Parkinson's disease. Cell Tissue Res. 373, 9–20.
Brahmachari, S., Ge, P., Lee, S.H., Kim, D., Karuppagounder, S.S., Kumar, M., Mao, X., Shin, J.H., Lee, Y., Pletnikova, O., Troncoso, J.C., Dawson, V.L., Dawson, T.M., Ko, H.S., 2016. Activation of tyrosine kinase c-Abl contributes to alpha-synuclein-induced neurodegeneration. J. Clin. Invest. 126, 2970–2988.
Brahmachari, S., Karuppagounder, S.S., Ge, P., Lee, S., Dawson, V.L., Dawson, T. M., Ko, H.S., 2017. C-abl and Parkinson's disease: mechanisms and therapeutic potential. J. Parkinsons Dis. 7, 589–601.
Brennan, A.M., Suh, S.W., Won, S.J., Narasimhan, P., Kauppinen, T.M., Lee, H., Edling, Y., Chan, P.H., Swanson, R.A., 2009. NADPH oxidase is the primary source of superoxide induced by NMDA receptor activation. Nat. Neurosci. 12, 857–863.
Chinta, S.J., Andersen, J.K., 2006. Reversible inhibition of mitochondrial complex I activity following chronic dopaminergic glutathione depletion in vitro: implications for Parkinson's disease. Free Radic. Biol. Med. 41, 1442–1448.
Clark, J., Clore, E.L., Zheng, K., Adame, A., Masliah, E., Simon, D.K., 2010. Oral N-acetyl-cysteine attenuates loss of dopaminergic terminals in alpha-synuclein overexpressing mice. PLoS One 5, e12333.
Cristovao, A.C., Guhathakurta, S., Bok, E., Je, G., Yoo, S.D., Choi, D.H., Kim, Y. S., 2012. NADPH oxidase 1 mediates alpha-synucleinopathy in Parkinson's disease. J. Neurosci. 32, 14465–14477.
Dauer, W., Przedborski, S., 2003. Parkinson's disease: mechanisms and models. Neuron 39, 889–909.
Deas, E., Cremades, N., Angelova, P.R., Ludtmann, M.H., Yao, Z., Chen, S., Horrocks, M.H., Banushi, B., Little, D., Devine, M.J., Gissen, P., Klenerman, D., Dobson, C.M., Wood, N.W., Gandhi, S., Abramov, A.Y., 2016. Alpha-synuclein oligomers interact with metal ions to induce oxidative stress and neuronal death in Parkinson's disease. Antioxid. Redox Signal. 24, 376–391.
Dexter, D.T., Sian, J., Rose, S., Hindmarsh, J.G., Mann, V.M., Cooper, J.M., Wells, F.R., Daniel, S.E., Lees, A.J., Schapira, A.H., et al., 1994. Indices of oxidative stress and mitochondrial function in individuals with incidental Lewy body disease. Ann. Neurol. 35, 38–44.
Fu, Y., Yuan, Y., Halliday, G., Rusznak, Z., Watson, C., Paxinos, G., 2012. A cytoarchitectonic and chemoarchitectonic analysis of the dopamine cell groups in the substantia nigra, ventral tegmental area, and retrorubral field in the mouse. Brain Struct. Funct. 217, 591–612.
Ghosh, S., Geahlen, R.L., 2015. Stress granules modulate SYK to cause microglial cell dysfunction in Alzheimer's disease. EBioMedicine 2, 1785–1798.
Gombash, S.E., Manfredsson, F.P., Kemp, C.J., Kuhn, N.C., Fleming, S.M., Egan, A.E., Grant, L.M., Ciucci, M.R., MacKeigan, J.P., Sortwell, C.E., 2013. Morphological and behavioral impact of AAV2/5-mediated overexpression of human wildtype alpha-synuclein in the rat nigrostriatal system. PLoS One 8, e81426.
Grassi, D., Howard, S., Zhou, M., Diaz-Perez, N., Urban, N.T., Guerrero-Given, D., Kamasawa, N., Volpicelli-Daley, L.A., LoGrasso, P., Lasmezas, C.I., 2018. Identification of a highly neurotoxic alpha-synuclein species inducing mitochondrial damage and mitophagy in Parkinson's disease. Proc. Natl. Acad. Sci. U. S. A. 115, E2634–E2643.
Hantschel, O., Superti-Furga, G., 2004. Regulation of the c-Abl and Bcr-Abl tyrosine kinases. Nat. Rev. Mol. Cell Biol. 5, 33–44.
Hebron, M.L., Lonskaya, I., Moussa, C.E., 2013. Nilotinib reverses loss of dopamine neurons and improves motor behavior via autophagic degradation of alpha-synuclein in Parkinson's disease models. Hum. Mol. Genet. 22, 3315–3328.
Imam, S.Z., Zhou, Q., Yamamoto, A., Valente, A.J., Ali, S.F., Bains, M., Roberts, J.L., Kahle, P.J., Clark, R.A., Li, S., 2011. Novel regulation of parkin function through c-Abl-mediated tyrosine phosphorylation: implications for Parkinson's disease. J. Neurosci. 31, 157–163.
Ip, C.W., Klaus, L.C., Karikari, A.A., Visanji, N.P., Brotchie, J.M., Lang, A.E., Volkmann, J., Koprich, J.B., 2017. AAV1/2-induced overexpression of A53T-alpha-synuclein in the substantia nigra results in degeneration of the nigrostriatal system with Lewy-like pathology and motor impairment: a new mouse model for Parkinson's disease. Acta. Neuropathol. Commun. 5, 11.
Karim, M.R., Liao, E.E., Kim, J., Meints, J., Martinez, H.M., Pletnikova, O., Troncoso, J.C., Lee, M.K., 2020. alpha-Synucleinopathy associated c-Abl activation causes p53-dependent autophagy impairment. Mol. Neurodegener. 15, 27.
Karuppagounder, S.S., Alin, L., Chen, Y., Brand, D., Bourassa, M.W., Dietrich, K., Wilkinson, C.M., Nadeau, C.A., Kumar, A., Perry, S., Pinto, J.T., Darley-Usmar, V., Sanchez, S., Milne, G.L., Pratico, D., Holman, T.R., Carmichael, S. T., Coppola, G., Colbourne, F., Ratan, R.R., 2018. N-acetylcysteine targets 5 lipoxygenase-derived, toxic lipids and can synergize with prostaglandin E2 to inhibit ferroptosis and improve outcomes following hemorrhagic stroke in mice. Ann. Neurol. 84, 854–872.
Ko, H.S., Lee, Y., Shin, J.H., Karuppagounder, S.S., Gadad, B.S., Koleske, A.J., Pletnikova, O., Troncoso, J.C., Dawson, V.L., Dawson, T.M., 2010. Phosphorylation by the c-Abl protein tyrosine kinase inhibits parkin's ubiquitination and protective function. Proc. Natl. Acad. Sci. U. S. A. 107, 16691–16696.
Langston, J.W., Ballard, P., Tetrud, J.W., Irwin, I., 1983. Chronic Parkinsonism in humans due to a product of meperidine-analog synthesis. Science 219, 979–980.
Lawana, V., Singh, N., Sarkar, S., Charli, A., Jin, H., Anantharam, V., Kanthasamy, A.G., Kanthasamy, A., 2017. Involvement of c-Abl kinase in microglial activation of NLRP3 inflammasome and impairment in autolysosomal system. J. Neuroimmune Pharmacol. 12, 624–660.
Lee, S., Kim, S., Park, Y.J., Yun, S.P., Kwon, S.H., Kim, D., Kim, D.Y., Shin, J.S., Cho, D.J., Lee, G.Y., Ju, H.S., Yun, H.J., Park, J.H., Kim, W.R., Jung, E.A., Lee, S., Ko, H.S., 2018. The c-Abl inhibitor, Radotinib HCl, is neuroprotective in a preclinical Parkinson's disease mouse model. Hum. Mol. Genet. 27, 2344–2356.
Mahul-Mellier, A.L., Fauvet, B., Gysbers, A., Dikiy, I., Oueslati, A., Georgeon, S., Lamontanara, A.J., Bisquertt, A., Eliezer, D., Masliah, E., Halliday, G., Hantschel, O., Lashuel, H.A., 2014. c-Abl phosphorylates alpha-synuclein and regulates its degradation: implication for alpha-synuclein clearance and contribution to the pathogenesis of Parkinson's disease. Hum. Mol. Genet. 23, 2858–2879.
Maiani, E., Diederich, M., Gonfloni, S., 2011. DNA damage response: the emerging role of c-Abl as a regulatory switch?. Biochem. Pharmacol. 82, 1269–1276.
Martin, H.L., Teismann, P., 2009. Glutathione--a review on its role and

significance in Parkinson's disease. FASEB J. 23, 3263–3272.
Martinez-Banaclocha, M.A., 2012. N-acetyl-cysteine in the treatment of Parkinson's disease. What are we waiting for?. Med. Hypotheses 79, 8–12.
Monti, D.A., Zabrecky, G., Kremens, D., Liang, T.W., Wintering, N.A., Cai, J., Wei, X., Bazzan, A.J., Zhong, L., Bowen, B., Intenzo, C.M., Iacovitti, L., Newberg, A. B., 2016. N-acetyl cysteine may support dopamine neurons in Parkinson's disease: preliminary clinical and cell line data. PLoS One 11, e0157602.
Monti, D.A., Zabrecky, G., Kremens, D., Liang, T.W., Wintering, N.A., Bazzan, A. J., Zhong, L., Bowens, B.K., Chervoneva, I., Intenzo, C., Newberg, A.B., 2019. N-acetyl cysteine is associated with dopaminergic improvement in Parkinson's disease. Clin. Pharmacol. Ther. 106, 884–890.
Musgrove, R.E., Helwig, M., Bae, E.J., Aboutalebi, H., Lee, S.J., Ulusoy, A., Di Monte, D.A., 2019. Oxidative stress in vagal neurons promotes parkinsonian pathology and intercellular alpha-synuclein transfer. J. Clin. Invest. 130, 3738–3753.
Nakamura, K., 2013. Alpha-synuclein and mitochondria: partners in crime?. Neurotherapeutics 10, 391–399.
Norris, E.H., Giasson, B.I., 2005. Role of oxidative damage in protein aggregation associated with Parkinson's disease and related disorders. Antioxid. Redox Signal. 7, 672–684.
Pagan, F.L., Wilmarth, B., Torres-Yaghi, Y., Hebron, M.L., Mulki, S., Ferrante, D., Matar, S., Ahn, J., Moussa, C., 2020. Long-term safety and clinical effects of nilotinib in Parkinson's disease. Mov. Disord..
Pinilla-Ibarz, J., Sweet, K., Emole, J., Fradley, M., 2015. Long-term BCR-ABL1 tyrosine kinase inhibitor therapy in chronic myeloid leukemia. Anticancer Res. 35, 6355–6364.
Rahimmi, A., Khosrobakhsh, F., Izadpanah, E., Moloudi, M.R., Hassanzadeh, K., 2015. N-acetylcysteine prevents rotenone-induced Parkinson's disease in rat: an investigation into the interaction of parkin and Drp1 proteins. Brain Res. Bull. 113, 34–40.
Reyes, R.C., Cittolin-Santos, G.F., Kim, J.E., Won, S.J., Brennan-Minnella, A.M., Katz, M., Glass, G.A., Swanson, R.A., 2016. Neuronal glutathione content and antioxidant capacity can be normalized in situ by N-acetyl cysteine concentrations attained in human cerebrospinal fluid. Neurotherapeutics 13, 217–225.
Rushworth, G.F., Megson, I.L., 2014. Existing and potential therapeutic uses for N-acetylcysteine: the need for conversion to intracellular glutathione for antioxidant benefits. Pharmacol. Ther. 141, 150–159.
Samuni, Y., Goldstein, S., Dean, O.M., Berk, M., 2013. The chemistry and biological activities of N-acetylcysteine. Biochim. Biophys. Acta 1830, 4117–4129.
Sandoval, I.M., Kuhn, N.M., Manfredsson, F.P., 2019. Multimodal production of adeno-associated virus. Methods Mol. Biol. 1937, 101–124.
Sasaki, A., Arawaka, S., Sato, H., Kato, T., 2015. Sensitive western blotting for detection of endogenous Ser129-phosphorylated alpha-synuclein in intracellular and extracellular spaces. Sci. Rep. 5, 14211.
Scudamore, O., Ciossek, T., 2018. Increased oxidative stress exacerbates alpha-synuclein aggregation in vivo. J. Neuropathol. Exp. Neurol. 77, 443–453.
Seaton, T.A., Cooper, J.M., Schapira, A.H., 1997. Free radical scavengers protect dopaminergic cell lines from apoptosis induced by complex I inhibitors. Brain Res. 777, 110–118.
Sharma, A., Kaur, P., Kumar, V., Gill, K.D., 2007. Attenuation of 1-methyl-4-phenyl-1, 2,3,6-tetrahydropyridine induced nigrostriatal toxicity in mice by N-acetyl cysteine. Cell. Mol. Biol. (Noisy-le-grand) 53, 48–55.
Sherer, T.B., Kim, J.H., Betarbet, R., Greenamyre, J.T., 2003. Subcutaneous rotenone exposure causes highly selective dopaminergic degeneration and alpha-synuclein aggregation. Exp. Neurol. 179, 9–16.
Shiotsuki, H., Yoshimi, K., Shimo, Y., Funayama, M., Takamatsu, Y., Ikeda, K., Takahashi, R., Kitazawa, S., Hattori, N., 2010. A rotarod test for evaluation of motor skill learning. J. Neurosci. Methods 189, 180–185.
Simon, D.K., Tanner, C.M., Brundin, P., 2020. Parkinson disease epidemiology, pathology, genetics, and pathophysiology. Clin. Geriatr. Med. 36, 1–12.
Simuni, T., Fiske, B., Merchant, K., Coffey, C.S., Klingner, E., Caspell-Garcia, C., Lafontant, D.E., Matthews, H., Wyse, R.K., Brundin, P., Simon, D.K., Schwarzschild, M., Weiner, D., Adams, J., Venuto, C., Dawson, T.M., Baker, L., Kostrzebski, M., Ward, T., Rafaloff, G., Parkinson Study Group, N.-P.D.I., Collaborators, 2020. Efficacy of nilotinib in patients with moderately advanced Parkinson disease: a randomized clinical trial. JAMA Neurol..
Sirvent, A., Benistant, C., Roche, S., 2008. Cytoplasmic signalling by the c-Abl tyrosine kinase in normal and cancer cells. Biol. Cell 100, 617–631.
Sun, X., Majumder, P., Shioya, H., Wu, F., Kumar, S., Weichselbaum, R., Kharbanda, S., Kufe, D., 2000. Activation of the cytoplasmic c-Abl tyrosine kinase by reactive oxygen species. J. Biol. Chem. 275, 17237–17240.
Tanner, C.M., Kamel, F., Ross, G.W., Hoppin, J.A., Goldman, S.M., Korell, M., Marras, C., Bhudhikanok, G.S., Kasten, M., Chade, A.R., Comyns, K., Richards, M.B., Meng, C., Priestley, B., Fernandez, H.H., Cambi, F., Umbach, D.M., Blair, A., Sandler, D.P., Langston, J.W., 2011. Rotenone, paraquat, and Parkinson's disease. Environ. Health Perspect. 119, 866–872.
Thakur, P., Breger, L.S., Lundblad, M., Wan, O.W., Mattsson, B., Luk, K.C., Lee, V.M.Y., Trojanowski, J.Q., Bjorklund, A., 2017. Modeling Parkinson's disease pathology by combination of fibril seeds and alpha-synuclein overexpression in the rat brain. Proc. Natl. Acad. Sci. U. S. A. 114, E8284–E8293.
Virel, A., Dudka, I., Laterveer, R., Af Bjerken, S., 2019. (1)H NMR profiling of the 6-OHDA parkinsonian rat brain reveals metabolic alterations and signs of recovery after N-acetylcysteine treatment. Mol. Cell. Neurosci. 98, 131–139.
Volpicelli-Daley, L.A., Luk, K.C., Lee, V.M., 2014. Addition of exogenous alpha-synuclein preformed fibrils to primary neuronal cultures to seed recruitment of endogenous alpha-synuclein to Lewy body and Lewy neurite-like aggregates. Nat. Protoc. 9, 2135–2146.
Wang, X., Becker, K., Levine, N., Zhang, M., Lieberman, A.P., Moore, D.J., Ma, J., 2019. Pathogenic alpha-synuclein aggregates preferentially bind to mitochondria and affect cellular respiration. Acta Neuropathol. Commun. 7, 41.
Watabe, M., Nakaki, T., 2007. Mitochondrial complex I inhibitor rotenone-elicited dopamine redistribution from vesicles to cytosol in human dopaminergic SH-SY5Y cells. J. Pharmacol. Exp. Ther. 323, 499–507.
Weisberg, E., Manley, P., Mestan, J., Cowan-Jacob, S., Ray, A., Griffin, J.D., 2006. AMN107 (nilotinib): a novel and selective inhibitor of BCR-ABL. Br. J. Cancer 94, 1765–1769.
Won, S.J., Kim, J.E., Cittolin-Santos, G.F., Swanson, R.A., 2015. Assessment at the single-cell level identifies neuronal glutathione depletion as both a cause and effect of ischemia-reperfusion oxidative stress. J. Neurosci. 35, 7143–7152.
Zeevalk, G.D., Razmpour, R., Bernard, L.P., 2008. Glutathione and Parkinson's disease: is this the elephant in the room?. Biomed. Pharmacother. 62, 236–249.
Zhou, L., Zhang, Q., Zhang, P., Sun, L., Peng, C., Yuan, Z., Cheng, J., 2017. c-Abl-mediated Drp1 phosphorylation promotes oxidative stress-induced mitochondrial fragmentation and neuronal cell death. Cell Death Dis. 8, e3117.